16TH EUROPEAN CONFERENCE ON EARTHQUAKE ENGINEERING THESSALONIKI 18 - 21 JUNE 2018

LOSS ASSESSMENT OF LIFELINE NETWORKS CONSIDERING THE EFFECT OF DAMAGE SPATIAL CORRELATION

Alireza GARAKANINEZHAD[1], Morteza BASTAMI[2]

ABSTRACT

Seismic loss assessment for a spatially distributed system, such as lifeline networks, depends on the distribution of ground-motion intensity measures (IMs) over region and the vulnerability of structure in the given region. The proper treatment of variability of both ground motion and structural vulnerability is essential. In particular, it has been shown that spatial correlation of both these parameters has an important impact. In recent years, some models have been proposed to quantify the spatial correlation of IMs; however, there is little attention to structure-to-structure damage correlation. In this paper, a methodology based on spatial statistics for considering this correlation in the network risk assessment is proposed. In this methodology, direct loss of structures imposed an earthquake event is considered as a random field whose cross-covariance function is presented using semivariogram functions. The parameters of the model can be estimated from spatial characterization of the expected loss of structures in each damage state. This framework is shown on a transportation network located in Tehran and the effect of damage correlation is investigated. The results indicate that spatial correlation of damage has a significant effect on risk estimate, especially may lead underestimation of risk assessment in rare event cases.

Keywords: Lifeline systems; Spatial correlation; Damage correlation; Reliability & Risk Analysis; Transportation networks

1. INTRODUCTION

Lifeline networks such as transportation networks, electrical networks, and water distribution networks play a significant role in the capability of a society to come back after a natural hazard like earthquake. In fact, the recovery activities are highly dependent on the performance of these networks during hazards. For this reason, estimation of the performance of lifelines received much attention. However, this estimation has accompanied highly uncertain. In general, spatial correlation of ground-motion intensity measure (IM) and the structural damage result in these uncertainties. These years, some researchers have proposed frameworks to incorporate correlation of both IMs and structures.
Several research works studied the effect of spatial correlation of ground-motion IMs on the loss estimation of lifeline networks. It is indicated that for rare events, ignoring spatial correlation of IMs may result in underestimation of the risk assessment, and overestimation in frequent events. In this way, models for different IMs (peak ground acceleration [PGA], peak ground velocity [PGV], peak ground displacement [PGD], and spectral accelerations [SAs]) are presented based on records from different regions. Boore et al. (2003) developed a spatial correlation model of PGA using 1994 Northridge earthquake observations. Wang and Takada (2005) presented a model of PGV using several earthquakes occurred in Japan and the 1999 Chi-Chi. Other studies, such as Goda and Hong (2008), Jayaram and Baker (2009), and Hong et al. (2009) used some well-recorded earthquakes to develop the spatial correlation model for different IMs. In these works, records of each event are

[1]Ph. D. student, International Institute of Earthquake Engineering and Seismology (IIEES), Tehran, Iran, a.garkani@iieess.ac.ir
[2]Associate Professor, International Institute of Earthquake Engineering and Seismology (IIEES), Tehran, Iran, m.bastami@iiees.ac.ir

investigated separately and the model is proposed based on the obtained results. In the other approach, spatial correlation models were computed using data gathering from several earthquakes. Goda and Atkinson (2010), Esposito and Iervolino (2011), Esposito and Iervolino (2012) and Garakaninezhad et al.(2017) proposed models for different IMs using collocated data from various regions.
The model for vector IMs have also been introduced. Loth and Baker (2013) and Du and Wang (2013) presented the cross-correlation model for SAs at multiple periods. Wang and Du, 2013 u proposed models for two sets of IMs, one foe PGA, PGV and Ia and one for SAs at multiple periods.
The impact of spatial correlation among structures has received less attention. This correlation may result from the similarity of design or construction methods and the material quality of structures in a network. Therefore, a simulation procedure which can consider these shared or uncorrelated qualities, is required to accurately risk assessment. In these years, researchers have focused on treatment of these spatial correlations. Lee and Kiremidjian (2007) presented framework which included the effects of correlations under a given earthquake scenario. Shiraki et al. (2007) investigated the total bridge network delay under a seismic hazard using user-equilibrim analysis. Bocchini and Frangopol (2011) presented a procedure to assess the correlation of the individual bridge damage levels. Dong and Frangopol (2017) presented a framework considering spatial correlation of IMs, vulnerability of bridges and links.
It is clear that it is of vital importance to propose a framework which accounts for structure damage correlation in addition to IMs correlation. However, based on aforementioned studies, frameworks which consider damage level correlation have received less attention. In this paper, a framework which considers correlation of both IMs and structures damage is proposed. In order to assess the hazard risk of spatially-distributed systems with the presence of structure-to-structure damage correlation, the ability of spatial correlation is used.
In the following section, spatial correlation is described. Section 3 presents the proposed framework. Finally, in section 4, the capability of the framework is illustrated on a transportation network in Tehran.

2. SPATIAL CORRELATION

The framework presented in this paper can incorporate spatial correlation in both simulated IMs and damage states. These simulations are done based on techniques proposed in spatial statistics. The spatial correlation of a random field can be consider using semivariogram which is widely used in geostatistics. The semivariogram for a second-order stationary random field can be written as

$$\gamma(\boldsymbol{h}) = \frac{1}{2} E\left[\left(Z_{u_i} - Z_{u_i+h}\right)^2\right] \quad (1)$$

where Z_{u_i} and Z_{u_i+h} are the value of random variables separated by the separation vector **h**. A random field is a second-order stationary if its mean value is identical across the domain and also, the two-point statistics depend only on the separation distance and not on their actual location. A stationary semivariogram is isotropic when it is not dependent on the directions. In this case, the separation vector **h** in Equation (1) can be replaced by separation distance *h*. Under these assumptions and based on the methods of moments, a classic estimation of semivariogram can be written as follows (Goovaerts 1997)

$$\hat{\gamma}(h) = \frac{1}{2N(h)} \sum_{\alpha=1}^{N(h)} \left[\left(Z_{u_\alpha} - Z_{u_\alpha+h}\right)^2\right] \quad (2)$$

where $\hat{\gamma}(h)$ denotes the empirical semivariogram and $N(h)$ denotes the number of data pairs separated by h. In isotropic and second-order stationary random field, the relation between semivariogram function and correlation function is defined as

$$\gamma(h) = C(0)\big(1 - \rho(h)\big) = Var(Z)\big(1 - \rho(h)\big) \quad (3)$$

where $\rho(h)$ and C denote the correlation function and the covariance function, respectively, which are defined as

$$\rho(h) = \frac{c(h)}{C(0)} \tag{4}$$

$$C(h) = Cov(Z_u, Z_{u+h}) = E\left(\left(Z_u - E(Z_u)\right)\left(Z_{u+h} - E(Z_{u+h})\right)\right) \tag{5}$$

There are models in the literature to present semivariogram theoretically. The most widely used models are the exponential, Gaussian, and spherical model (Goovaerts 1997). The exponential model which is applied by several researchers to approximate the empirical semivariogram data is defined as

$$\gamma(h) = a\left[1 - e^{(-\frac{3h}{b})}\right] \tag{6}$$

where a denotes the sill of the semivariogram which is equal to the variance of empirical data and b is the range of the semivariogram which is defined as the separation distance when the semivariogram reaches 0.95 times the sill.

3. RISK ASSESSMENT FRAMEWORK

The proposed framework includes several steps and its flowchart is depicted in Figure 1. In the first step, inventory of the network and characteristics of active faults in the region should be identified. Based on the seismic source model, a set of earthquake scenarios is generated and for each structure in the network the considered IM is predicted. Then, the correlated damage amps for each type of bridge are simulated using semivariogram given correlation range of damage sate. Finally, the performance of the network is computed based on the generated damage maps.

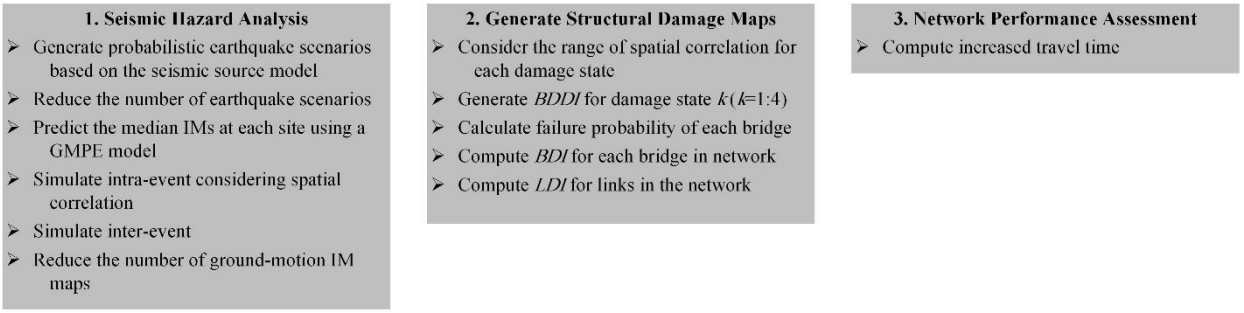

Figure 1. Flowchart of the proposed framework

3.1 Seismic hazard analysis

The aim of this step is to simulate a set of probabilistic earthquake scenarios and associated ground motion intensity maps. The set of scenarios are simulated using a seismic source model which is obtained from seismicity of the region. The number of earthquake scenarios is considerable, hence it is reasonable to use methods to reduce the computational costs. Researchers proposed methods to select the reduced set of scenarios. These approaches can be classified into user-defined approach (Chang et al. 2000, Shiraki et al. 2007 and Campbell and Seligson 2003), approaches based on importance sampling (Kiremidjian et al. (2007) and Jayaram and Baker (2010)) or ground motion contributors (Han and Davidson 2012).
Next, for each earthquake scenario, the considered IMs can be predicted at each location using a ground-motion prediction equation (GMPE) model. The general form of GMPE is as follows

$$ln(Y_{sq}) = ln\,\bar{Y}_{sq}(M, R, \theta) + \varepsilon_{sq} + \eta_q \tag{7}$$

Where Y_{sq}, is the considered IM at site *s* and triggered by earthquake *q*, $\bar{Y}_{sq}(M,R,\theta)$ denotes the predicted mean value of ground-motion intensity, *M* presents earthquake magnitude, *R* is the site-to-source distance, and θ shows the other parameters, such as local site conditions and faulting mechanism. ε_{sq} and η_q indicate the intra- and inter-event residuals, respectively. These terms are assumed to be normal variables with zero mean and standard deviations of σ_{sq} and τ_q, respectively (Jayaram and Baker 2008). Spatial correlation of IMs under an earthquake scenario among structure locations is simulated by intra-event residuals. The residuals are generated using a spatially-correlated multivariate normal distribution.

The intra-event residual should be simulated based on a spatially-correlated multivariate normal distribution and the inter-event residual based on a univariate normal distribution. Most of the spatial correlation models, mentioned in Section 2, used the exponential form such as Equation 6. In general, these models consider sill (*a*) equal to 1 and the correlation range (*b*) is presented as a function of period. In order to consider anisotropy, the correlation range should be modified with anisotropy ratio which proposed in Garakaninezhad and Bastami (2017). Then, the intra-event residuals can be simulated using the obtained correlation model as a function of distance.

In addition to reduce the number of scenario, the reduced set of ground-motion IM maps can also be selected. Vaziri et al. (2012) and Han and Davidson (2012) proposed methods based on optimization and considering hazard curves.

3.2 Seismic vulnerabilities of bridges and links

Estimating seismic risk of a transportation network requires assessing the structural performance level of structures in the network. The structural performance is generally obtained from fragility functions. A fragility function of bridge *k*, determines the exceedance probability of a damage state with a given the intensity of the seismic ground motion. This function can be written as

$$P\left(DS_{k_r} \geq ds|IM\right) = \Phi\left(\frac{ln(IM)-ln(im_r)}{\beta_r}\right) \quad (8)$$

where im_r presents the median value of IM of damage state r; β_r denotes the standard deviation of the logarithmic of ground-motion intensity associated with the damage state, and [Φ] is the standard normal cumulative distribution function. Under a given IM, the probability of an individual structure *k* being in a damage state *r* is obtained from the difference between the exceedance probabilities of damage state *r* and *r+1*. The expected bridge damage index (BDI_k) is defined as multiplying $P\left(DS_{k_r} \geq ds|IM\right)$ for each damage state *r* with the corresponding component damage state index ($BDDI_k$). Hence, BDI_k can be written as follows

$$BDI_k = \sum_{r=1}^{n_{DS}} BDDI_k . P\left(DS_{k_r} \geq ds|IM\right) \quad (9)$$

where n_{DS} is the number of damage states.

The components are connected by elements which is considered as links. Therefore, the performance of a link depends on components are at the each side of the given link. The link damage index can be written

$$LDI = \sqrt{\sum_{j=1}^{n_b}\left(BDI_j\right)^2} \quad (10)$$

where n_b presents the number of bridges on the link, and BDI_j is referred to bridges located on the either side of the link.

3.2.1 Simulation of damage correlation maps

Fragility functions account for different structural properties such as material type, linear and nonlinear material models, joint types and the other parameters. Since the response of an individual structure in a single ground-motion spectral acceleration (for example SA (at T=1.0 sec) for bridges in

a transportation network) may not be sufficient for explaining its performance, the structural response of a component can differ from the value determined by fragility function. This difference may be due to the variability of design or construction methods, or the material quality. Therefore, a simulation procedure which can consider these shared or uncorrelated qualities is required to accurately assess seismic risk. In order to compute BDI_k (Equation 9), it is required to generate a spatial random field of $BDDI_r$ given a damage state r. In this way, mean and covariance function are required. (Shiraki, Shinozuka, Moore, Chang, Kameda, and Tanaka 2007) proposed lognormal distribution for *BDDI* with means of 0.1, 0.3, 0.75 and 1 for different damage states of slight, moderate, major, and complete, respectively. The covariance function can be obtained from the exponential semivariogram model as presented in Section 2 with a given correlation range. In this study, this correlation range is considered equal for different damage states.

3.3 Network performance indicator

In the literature, several indicators have been proposed to assess the network performance. In general, these indicators analyse vulnerability, connectivity, or serviceability of the damaged network. For power networks, several indicators such as power system flow (Bastami 2007), connectivity (Dueñas-Osorio et al. 2007), serviceability ratio (Adachi and Ellingwood 2008), and recovery time (Shinozuka et al. 2007) have been proposed. For water networks, the researchers have introduced several indicators such as system serviceability measure (Wang and O'Rourke 2006), loss connectivity, serviceability ratio (Adachi and Ellingwood 2008), and damage consequence measure (Wang et al. 2010). Some indicators to evaluate transportation network performance are connectivity (Basöz and Kiremidjian 1995, Rokneddin et al. 2013), the percentage of bridges damaged (Shinozuka et al. 2007), increasing travel time (Jayaram and Baker 2010, Han and Davidson 2012), and mode destination accessibility (Handy and Niemeier 1997).
In this study, the serviceability analysis, which considers travel time increasing after an earthquake, is used. This indicator can be defined as

$$S = \sum_{i \in l} \sum_{j \in l} \int_0^{f_{ij}} t_{ij}(f) df \tag{11}$$

where, i and j denote nodes of the network, f_{ij} presents the traffic flow from node i to j in highway segment, t_{ij} is the time to trip between two given nodes.

4. ILLUSTRATIVE EXAMPLE

The framework is demonstrated on a transportation network which is located in Tehran, the capital of Iran, as an earthquake-prone region. The bridges and highways in the network are shown in Figure 2.

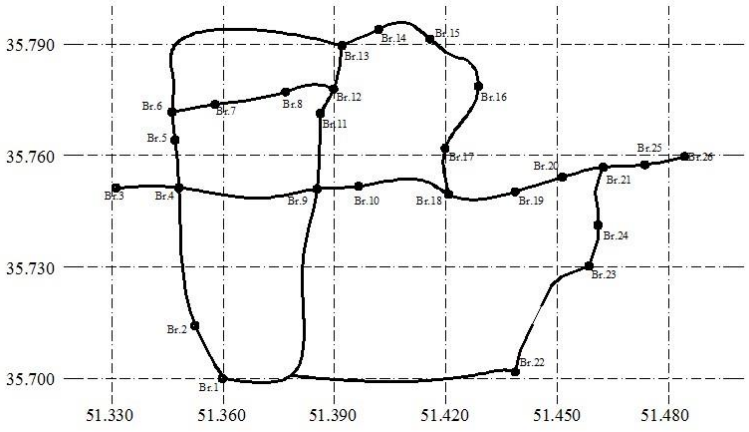

Figure 2. Layout of the considered transportation network

4.1 Seismic hazard assessment

The regional seismic hazard analysis consists of two main steps. First, based on a seismic source model, a set of probabilistic scenarios is generated and then, for each scenario, using a GMPE model the ground motion intensity is computed. The seismic rupture sources in the region are shown in Figure 3 and their characteristics are summarized in Table 1. In this study, the seismic source model presented by Tavakoli and Ghafory-Ashtiany (1999) is used. They divided Iran into 20 seismotectonic provinces, as shown in Figure 4, and Tehran is located in the 15th province. They presented coefficients of the Gutenberg-Richter relationship ($\log N = a - b \times m$) for all seismotectonic provinces. The coefficients a and b for Tehran are 1.0908 and 0.52, respectively. Based on the seismic model of sources, a reduced set of 100 earthquake scenarios are selected by using the optimization method presented by Vaziri et al. (2012).

The ground motion intensities (PGA, SAs at 0.3 and 1.0 sec) are computed using GMPE model developed by Akkar et al. (2014). For each event, the intra-event residuals are generated and spatial correlation among sites is modeled using the exponential function proposed by Garakaninezhad et al. (2017). The correlation range, b in Equation 6, as a function of period is shown in Figure 5. In this paper, the correlation ranges for PGA, SA(T=0.3 s), and SA(T=1.0 s) are 16 km, 21 km, and 14.9 km, respectively.

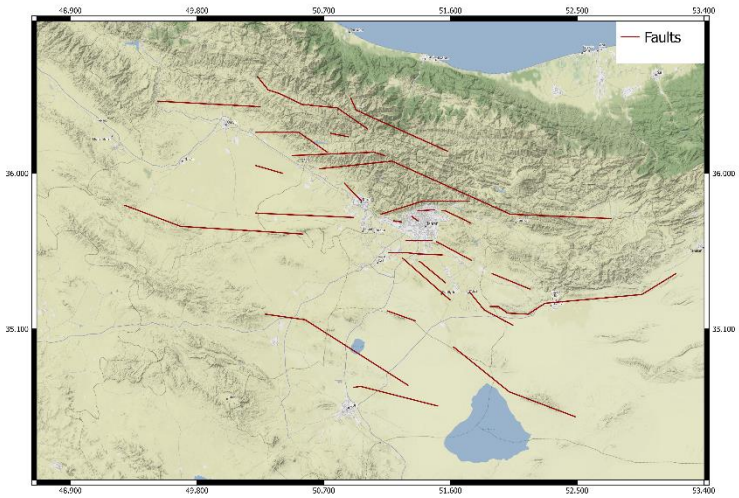

Figure 3. Faults over the considered region (Berberian, et al. 1993)

Table 1. Additional information of faults in the considered region

No.	Fault	Length (km)	M_{max}(Nowroozi 1985)	Type
1	Mosha	200	7.5	Thrust-Inverse
2	Pishva	34	6	Thrust-Inverse
3	South Rey	18.5	6.2	Thrust-Inverse
4	North Rey	17	6.1	Thrust-Inverse
5	Niavaran	13	6	Thrust-Inverse
6	North Tehran	75	6.9	Thrust-Inverse
7	Kahrizak	40	6.6	Thrust-Inverse
8	Garmsar	70	6.9	Thrust-Inverse

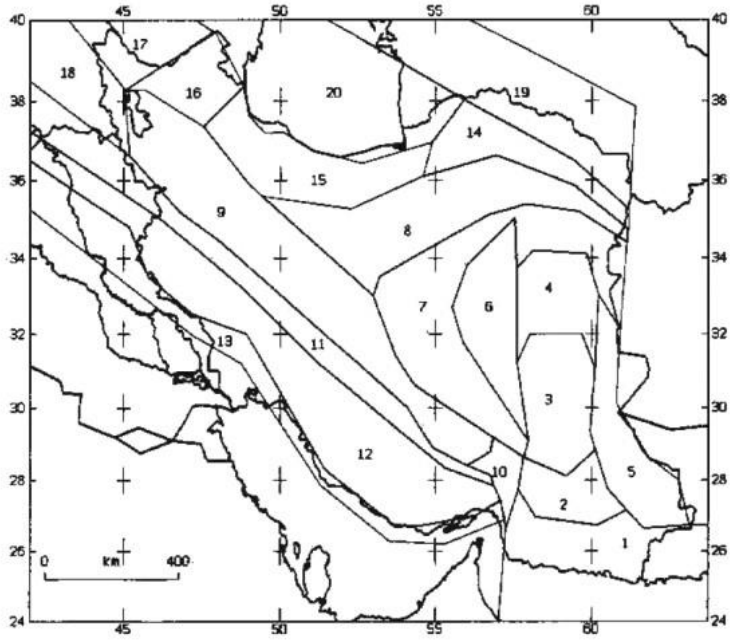

Figure 4. Seismic province of Iran (Tavakoli and Ghafory-Ashtiany 1999)

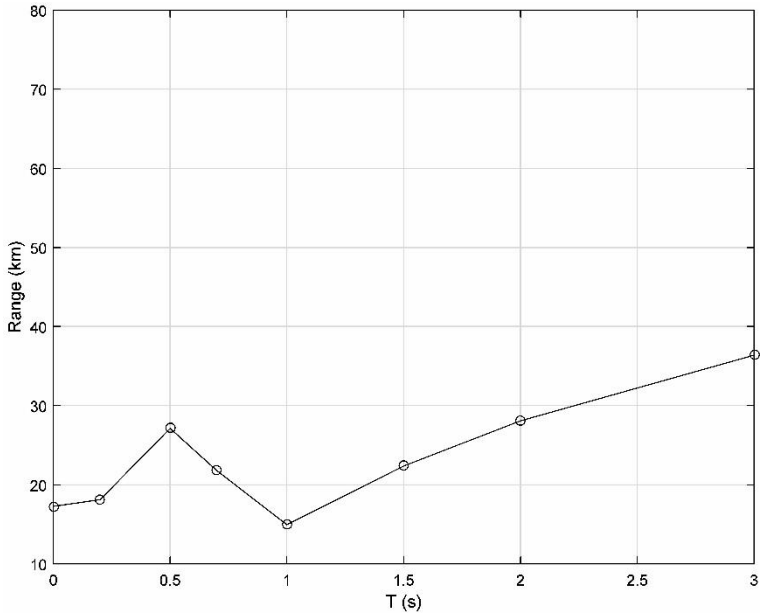

Figure 5. Correlation range as function of period (Garakaninezhad et al. 2017)

4.2 Seismic vulnerability assessment of bridges and links

In the proposed method, the damage correlation among bridges is considered in $BDDI_r$ simulation step. $BDDI_r$ should be simulated for each damage state, r, and for each type of bridges. In this study, it is assumed the type of all bridges are the same, hence $BDDI_r$ is simulated for four damage states. For each damage state, it is required to define the marginal distribution, mean and covariance matrix. The random field of $BDDI_r$ is assumed as lognormal random field with means proposed by Shiraki, Shinozuka, Moore, Chang, Kameda, and Tanaka 2007 for different damage states. In order to determine the covariance function, first, the correlation ranges of damage states are assumed, then using the semivariogram function (Equation 6) the covariance matrix is computed. In order to investigate the effect of correlation, four correlation ranges of 1, 4, 8, and 14 km are considered. The random fields obtained from these ranges indicate the effect of increasing correlation on the network

performance.

4.3 Network performance

The ratio of travel time between two cases of undamaged and damaged network is considered to evaluate the performance network. This performance is assessed under 100 earthquake scenarios, which are selected based on optimization approach, and four correlation ranges. Given an earthquake scenario and the covariance matrix associated with the considered correlation range, 1000 *BDDI* for slight, moderate, major and complete damage state are simulated. Then, BDI_k for bridge k can be obtained from multiplying the probability of being bridge in given damage state and the value of $BDDI_r$. Finally, using the obtained *BDI* of each damage state, the network performance can be assessed. Figure 6 indicates the ratio of travel time for four correlation range. As it can be seen, for frequent events the correlation of damage may lead overestimation of risk, however increasing the correlation range of damage can lead to increase the risk estimation for rare events.

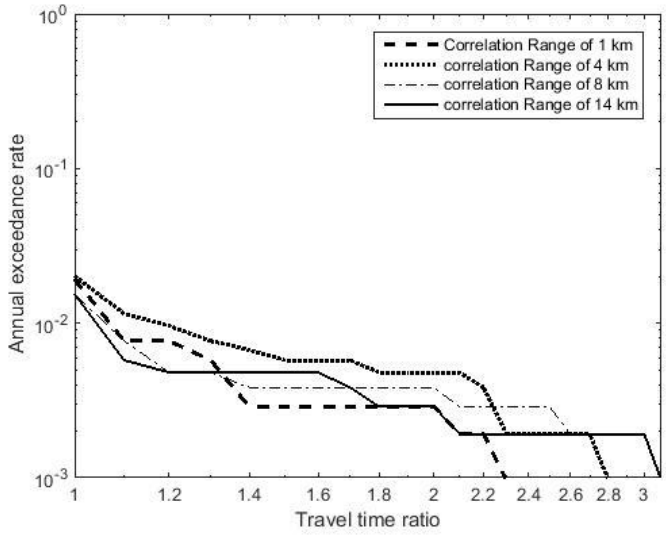

Figure 6. Travel time ratio for 4 ranges of damage correlation

5. CONCLUSION

In this paper, a framework for seismic risk assessment of transportation network is presented. This framework accounts for bridge-to-bridge spatial correlation in addition to spatial correlation among ground-motion intensity. The spatial correlation among bridges is considered in the simulation of bridge damage index for each damage state as a random field. The covariance of this random field can be obtained from the semivariogram function given a correlation range. Finally, using the simulated random field, the network performance can be assessed.
The approach is illustrated on the transportation network located in Tehran. The ratio of travel time between undamaged and damaged network is considered. The results show that increasing the damage correlation may lead to decrease the performance of the network. The framework is shown on the transportation network, however, it can be applied to the other lifeline networks.

6. ACKNOWLEDGEMENTS

The authors would like to acknowledge International Institute of Earthquake Engineering and Seismology (IIEES) for its help in providing research documents and Grant Number 7541.

7. REFERENCES

Adachi T, Ellingwood B R (2008). Serviceability of earthquake-damaged water systems: Effects of electrical power availability and power backup systems on system vulnerability. *Reliability engineering & system safety*, 93 (1): 78-88.

Akkar S, Sandıkkaya M, Bommer J (2014). Empirical ground-motion models for point-and extended-source crustal earthquake scenarios in Europe and the Middle East. *Bulletin of Earthquake Engineering*, 12 (1): 359-387.

Basöz N, Kiremidjian A (1995). A bridge prioritization method based on transportation system performance using GIS, in *Proceedings of the 6th US-Japan Workshop on Earthquake Disaster Prevention for Lifeline Systems, Tsukuba Science City, Japan*, 437-449.

Bastami M (2007). Seismic reliability of power supply system based on probabilistic approach, PhD thesis, Kobe University, Japan.

Berberian M, Ghoreishi M, Arzang Ravesh B, Mohajer Ashjaee A (1993). Seismotectonic and earthquake fault hazard investigations in the Tehran region. *Geological Survey of Iran, Tehran, Iran, Report*, (56).

Bocchini P, Frangopol D M (2011). A stochastic computational framework for the joint transportation network fragility analysis and traffic flow distribution under extreme events. *Probabilistic Engineering Mechanics*, 26 (2): 182-193.

Boore D M, Gibbs J F, Joyner W B, Tinsley J C, Ponti D J (2003). Estimated ground motion from the 1994 Northridge, California, earthquake at the site of the Interstate 10 and La Cienega Boulevard bridge collapse, West Los Angeles, California. *Bulletin of the Seismological Society of America*, 93 (6): 2737-2751.

Campbell K W, Seligson H A (2003). Quantitative method for developing hazard-consistent earthquake scenarios, in *Advancing Mitigation Technologies and Disaster Response for Lifeline Systems*, 829-838.

Chang S E, Shinozuka M, Moore J E (2000). Probabilistic earthquake scenarios: extending risk analysis methodologies to spatially distributed systems. *Earthquake Spectra*, 16 (3): 557-572.

Dong Y, Frangopol D M (2017). Probabilistic assessment of an interdependent healthcare–bridge network system under seismic hazard. *Structure and Infrastructure Engineering*, 13 (1): 160-170.

Du W, Wang G (2013). Intra-event spatial correlations for cumulative absolute velocity, arias intensity, and spectral accelerations based on regional site conditions. *Bulletin of the Seismological Society of America*, 103 (2A): 1117-1129.

Dueñas-Osorio L, Craig J I, Goodno B J (2007). Seismic response of critical interdependent networks. *Earthquake engineering & structural dynamics*, 36 (2): 285-306.

Esposito S, Iervolino I (2011). PGA and PGV spatial correlation models based on European multievent datasets. *Bulletin of the Seismological Society of America*, 101 (5): 2532-2541.

Esposito S, Iervolino I (2012). Spatial correlation of spectral acceleration in European data. *Bulletin of the Seismological Society of America*, 102 (6): 2781-2788.

Garakaninezhad A, Bastami M (2017). A novel spatial correlation model based on anisotropy of earthquake ground-motion intensity. *Bulletin of the Seismological Society of America*, Accepted.

Garakaninezhad A, Bastami M, Soghrat M R (2017). Spatial correlation for horizontal and vertical components of acceleration from northern Iran seismic events. *Journal of Seismology*, 1-12.

Goda K, Atkinson G M (2010). Intraevent spatial correlation of ground-motion parameters using SK-net data. *Bulletin of the Seismological Society of America*, 100 (6): 3055-3067.

Goda K, Hong H (2008). Spatial correlation of peak ground motions and response spectra. *Bulletin of the Seismological Society of America*, 98 (1): 354-365.

Goovaerts P (1997). Geostatistics for natural resources evaluation, Oxford University Press on Demand.

Han Y, Davidson R A (2012). Probabilistic seismic hazard analysis for spatially distributed infrastructure. *Earthquake Engineering & Structural Dynamics*, 41 (15): 2141-2158.

Handy S L, Niemeier D A (1997). Measuring accessibility: an exploration of issues and alternatives. *Environment and planning A*, 29 (7): 1175-1194.

Hong H, Zhang Y, Goda K (2009). Effect of spatial correlation on estimated ground-motion prediction equations. *Bulletin of the Seismological Society of America,* 99 (2A): 928-934.

Jayaram N, Baker J W (2008). Statistical tests of the joint distribution of spectral acceleration values. *Bulletin of the Seismological Society of America,* 98 (5): 2231-2243.

Jayaram N, Baker J W (2009). Correlation model for spatially distributed ground-motion intensities. *Earthquake Engineering & Structural Dynamics,* 38 (15): 1687-1708.

Jayaram N, Baker J W (2010). Efficient sampling and data reduction techniques for probabilistic seismic lifeline risk assessment. *Earthquake Engineering & Structural Dynamics,* 39 (10): 1109-1131.

Kiremidjian A S, Stergiou E, Lee R (2007). Issues in seismic risk assessment of transportation networks, in *Earthquake geotechnical engineering*, Springer, 461-480.

Lee R, Kiremidjian A S (2007). Uncertainty and correlation for loss assessment of spatially distributed systems. *Earthquake Spectra,* 23 (4): 753-770.

Loth C, Baker J W (2013). A spatial cross-correlation model of spectral accelerations at multiple periods. *Earthquake Engineering & Structural Dynamics,* 42 (3): 397-417.

Nowroozi A A (1985). Empirical relations between magnitudes and fault parameters for earthquakes in Iran. *Bulletin of the Seismological Society of America,* 75 (5): 1327-1338.

Rokneddin K, Ghosh J, Dueñas-Osorio L, Padgett J E (2013). Bridge retrofit prioritisation for ageing transportation networks subject to seismic hazards. *Structure and Infrastructure Engineering,* 9 (10): 1050-1066.

Shinozuka M, Dong X, Chen T, Jin X (2007). Seismic performance of electric transmission network under component failures. *Earthquake engineering & structural dynamics,* 36 (2): 227-244.

Shiraki N, Shinozuka M, Moore J E, Chang S E, Kameda H, Tanaka S (2007). System risk curves: Probabilistic performance scenarios for highway networks subject to earthquake damage. *Journal of Infrastructure Systems,* 13 (1): 43-54.

Tavakoli B, Ghafory-Ashtiany M (1999). Seismic hazard assessment of Iran. *Annals of Geophysics,* 42 (6).

Vaziri P, Davidson R, Apivatanagul P, Nozick L (2012). Identification of optimization-based probabilistic earthquake scenarios for regional loss estimation. *Journal of Earthquake Engineering,* 16 (2): 296-315.

Wang M, Takada T (2005). Macrospatial correlation model of seismic ground motions. *Earthquake spectra,* 21 (4): 1137-1156.

Wang Y, Au S-K, Fu Q (2010). Seismic risk assessment and mitigation of water supply systems. *Earthquake Spectra,* 26 (1): 257-274.

Wang Y, O'Rourke T D (2006). Seismic performance evaluation of water supply systems.